PHYSICAL REVIEW B **69**, 201103(R) (2004)

# Kondo resonance of single Co atoms embedded in Cu(111)

N. Quaas, M. Wenderoth, A. Weismann, and R. G. Ulbrich
*IV. Physikalisches Institut, Georg-August-Universität Göttingen, Tammannstrasse 1, D-37077 Göttingen, Germany*

K. Schönhammer
*Institut für Theoretische Physik, Georg-August-Universität Göttingen, Tammannstrasse 1, D-37077 Göttingen, Germany*

(Received 10 February 2004; revised manuscript received 24 March 2004; published 25 May 2004)

The Kondo resonance of single Co atoms embedded in a Cu matrix has been investigated with tunneling spectroscopy at $T=8$ K. Dilute magnetic alloys were prepared by homoepitaxial growth of Cu(111) films incorporating approximately 0.1% Co atoms as magnetic scattering centers. The Co impurities in the first layer of the Cu matrix show a characteristic, symmetric dip in the differential conductance around zero bias, indicating the presence of the many-body Abrikosov-Suhl resonance. The corresponding Kondo temperature is found to be $T_K=405\pm35$ K, which is much higher than previously reported values for Co adsorbate atoms.

DOI: 10.1103/PhysRevB.69.201103 PACS number(s): 72.15.Qm, 68.37.Ef, 73.20.At, 72.10.Fk

Nonmagnetic host metals with a dilute concentration of transition-metal impurities show an unusual asymptotic low-temperature behavior in many of their physical properties.[1] A prominent anomaly is the increase in resistivity with decreasing temperature below a characteristic value $T_K$. A theoretical explanation given by Kondo in 1964 recognized that resonant spin-flip scattering is the origin of the peculiar behavior of the alloys,[2] and was followed by steady theoretical research. Kondo systems have recently gained new attention, since local probe methods allow us to investigate *isolated* impurities with high spatial resolution in experiment.[3,4] Magnetic impurity atoms at the surface of noble metals are directly accessible with a scanning tunneling microscopy (STM) tip, and atomic-scale resolution for single Kondo systems on a surface has been achieved at low temperatures. Until now, scanning tunneling spectroscopy (STS) work has been focused on isolated $3d$- and $4f$-impurity atoms *adsorbed* on noble-metal surfaces. Several material combinations have been examined,[3–8] but only some of the adsorbed impurities have shown a clear Kondo-resonance feature in the tunneling spectra. The most characteristic fingerprint of the Kondo effect, recorded with the tip on top of the impurity atom, is a small and narrow dip in the differential conductance at zero bias. In the special case of a Co adsorbate atom on the Cu(111) surface, a slightly asymmetric dip has been observed independently in two previous STS studies.[6,7] The width of this feature is directly related to the Kondo temperature $T_K$ of the system. In comparison with the Kondo temperature $T_K^{\mathrm{bulk}}\sim500$ K determined with macroscopic methods,[1] the value for Co adsorbates was found to be very small ($T_K<100$ K).[7] According to the defining relation[9]

$$T_K=T_0\exp\left(-\frac{1}{|J|\rho_0(\vec{r})}\right), \tag{1}$$

the Kondo temperature of a single impurity is decisively determined by $\rho_0(\vec{r})=\rho(E_F,\vec{r})$, the local density of states (LDOS) at the Fermi-energy $E_F$ and the position $\vec{r}$. $|J|$ denotes the effective exchange interaction between the localized spin and the spins of the conduction electrons. It was proposed by Knorr *et al.* that adsorbed Kondo impurities, as probed in their STS experiments, should constitute a system with a reduced $|J|\rho_0(\vec{r})$.[7] According to Eq. (1), this leads to a lower $T_K$ than that obtained from macroscopic resistivity in bulk samples. The coordination number of impurities embedded in the surface layer is only slightly reduced compared with the bulk location, but considerably higher than in the adsorbate case. Thus, the Kondo temperature of an impurity atom embedded in the host's first crystal layer is expected to be higher than that of an adsorbed atom sitting on top of the first layer.

In the present work, single embedded Kondo impurities were studied with low-temperature STS. Small amounts of Co atoms were added via coevaporation to a thin Cu film grown epitaxially at room temperature on a Cu(111) single-crystal substrate. Our sample preparation closely approximates a bulk Kondo system, which is accessible for the surface-sensitive STS technique. The determination of $T_K$ for adsorbates using STS has been rather precise, while the bulk value of $T_K$ is not very accurately known. Therefore, it is desirable to measure the Kondo temperature of *embedded* Co in the Cu surface locally by STS. Our study of embedded impurities provides new information on the connection between microscopic and macroscopic experiments involving the Kondo effect.

The experiments were performed using a liquid $^4$He-cooled low-temperature UHV-STM operating at a temperature of 8 K. Special care was taken to also have the tip coupled efficiently to the cryostat. The base pressure of the UHV system was better than $1\times10^{-10}$ mbar at room temperature. Tunneling tips were electrochemically etched from tungsten wire and, after transfer to UHV, annealed and sputter-cleaned with 4 keV $Ar^+$ ions in a preparation chamber. During the experiments, the performance of the tip was tuned by controlled tip-sample contact and voltage pulses. The thin-film sample preparation was preceeded by sputtering and annealing cycles of the Cu(111) substrate at a base pressure of $5\times10^{-11}$ mbar. To avoid contamination, the clean crystal was removed *in situ* and locked away in the microscope chamber while degassing the Co and Cu *e*-beam

 

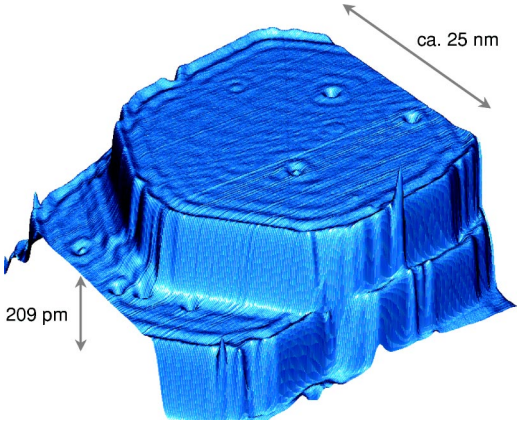


FIG. 1. (Color online) Constant current image of a RT-grown Cu film with a Co-alloyed surface in a 3D view (raw data from the microscope at $U_B = 0.3$ V, $I_T = 0.6$ nA). On the terraces and islands, standing-wave patterns of the surface-state electrons are visible together with a number of atomic defects located in the surface and subsurface crystal layers.

evaporators for several hours in the preparation chamber. Then, with the Cu(111) substrate held at room temperature, a 5-nm-thick Cu film was deposited at a rate of 0.04 ML/s. According to the desired Co concentration of 0.1%, the second evaporator simultaneously added a small amount of Co atoms to the growing film. This preparation procedure was performed identically for several films; only the amount and the distribution of the Co impurities was slightly varied from sample to sample. Only in a few cases are the atomic defects seen in the STM images due to noncobalt residual impurities. The purity of the base materials (Cu: 99.999%; Co: 99.99%) indicates that the percentage of non-Co defects is determined by the purity of the Cu and should be below 1% of all visible defects.

All of the cryogenic STM measurements were done with the tip stabilized in constant current mode. The spectroscopic data were acquired by additionally recording an $I(U)$ curve at every point with interrupted feedback loop. Further data processing included averaging and numerical differentiation. This provides a complete set of $dI/dU$ spectra as a function of the lateral coordinates on the Cu(111) surface.

A typical constant current image of the dilute Co-Cu films is shown in Fig. 1. Terraces and islands of sixfold symmetry with rounded corners are seen as a result of the room-temperature (RT) deposition process. Standing-wave patterns of the two-dimensional (2D) surface-state electrons are visible as pm-scale modulations in the tip height. Strong scattering is observed at steps and island edges, but also at several atomic defects in the surface. The height scale shows that there are no adsorbates present on the terraces, which would produce 80-pm-high bumps in constant current mode.[7] Therefore, the atomic scatterers that are seen here are located *in* or *below* the crystal surface. The spherical wave patterns indicate the lateral positions of the Co impurities within the Cu matrix. Furthermore, Fig. 1 also shows that more than only one type of atomic defect pattern is observed. Four distinct, characteristic patterns found on these surfaces are displayed in Fig. 2 together with their constant current

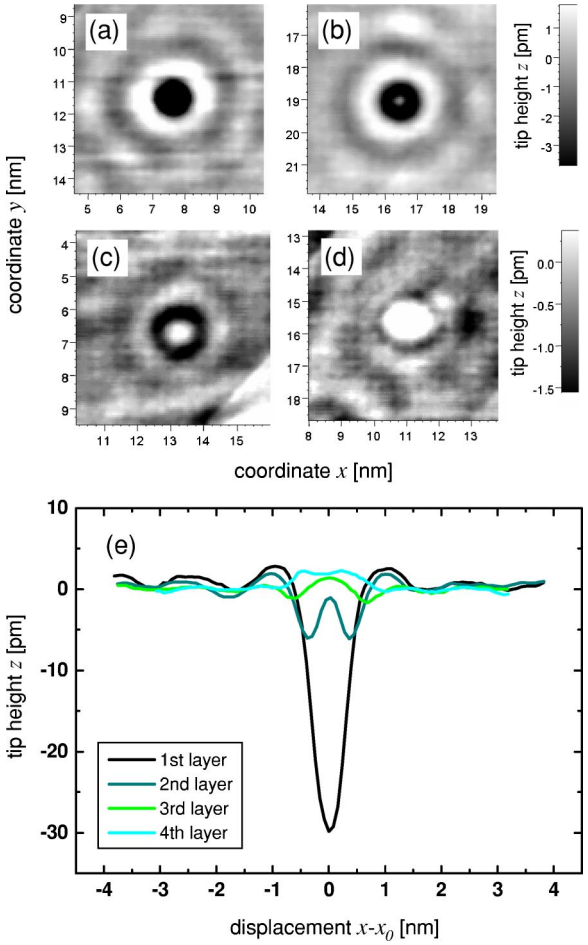


FIG. 2. (Color online) Four typical defect patterns in constant current mode ($U_B = 0.3$ V, $I_T = 0.6$ nA) of near-surface Co impurities in Cu(111). Corresponding cross sections are shown below. The vertical positions of the impurities are assigned as follows: (a) surface layer; (b) second layer; (c) third layer; (d) fourth layer.

cross sections. They indicate a tendency of the central tip height to increase from (a) to (d). Defect (a) (black line) shows a $\Delta z(0) = -30$ pm depression in constant current mode, which is understood as the suppression of the surface-state LDOS as it is expected for a surface-layer impurity atom. The spectroscopic results discussed in the following corroborate the assignment of pattern (a) to Co atoms embedded in the topmost surface layer of Cu(111). In contrast, the three other sections in Fig. 2 belong to defect patterns that we assign to Co atoms lying below the surface in the second, third, or even deeper crystal layers. This ordering is supported by STS on a third-layer pattern revealing the presence of a shifted surface-state band, which proves that it originates from a buried atomic scatterer. We thus find that the scattering of the surface state at these subsurface defect atoms produces a much stronger amplitude in constant current imaging than was expected from a previous theoretical treatment of surface-state scattering at buried impurities.[10]

Beyond imaging, single near-surface defects were also simultaneously characterized with spatially resolved STS. The constant current trace of such a scan is displayed in Fig. 3. Panel (c) exhibits four embedded atomic impurities, which

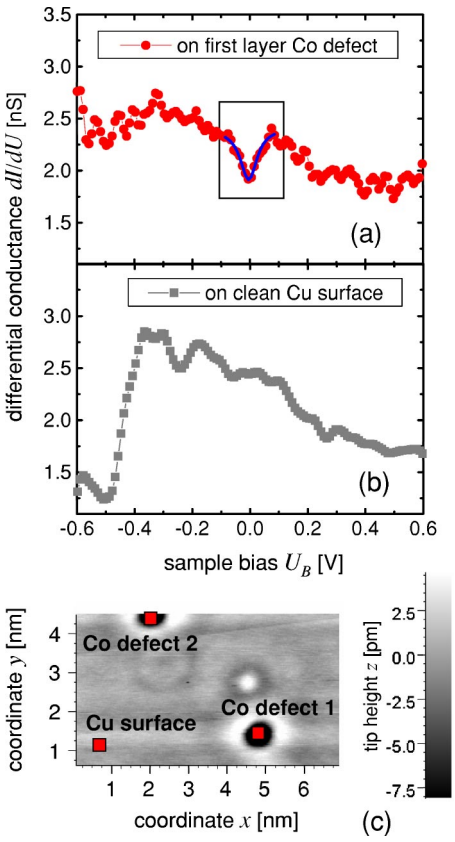


FIG. 3. (Color online) Spatially resolved tunneling spectroscopy of surface-layer Co defect atoms in Cu(111) (setpoint: $U_B = 0.5$ V, $I_T = 1.0$ nA). In (a), the averaged $dI/dU$ spectrum of defects 1 and 2 shows a dip around zero bias. The surface state which is present on the clean surface shown in (b) is absent in the defect spectra. The positions corresponding to the spectra are indicated by the squares in (c).

have distinct appearances corresponding to different depths relative to the surface. The two identical impurities, located to the upper left and to the lower right, are identified as Co atoms embedded in the surface layer. The spectra taken at both of these impurity positions are averaged and plotted in (a). They show a $dI/dU$ spectrum markedly different from that taken on the plain Cu surface indicated by (b). The $dI/dU$ spectra represent 49 single $I(U)$ spectra that were averaged at each impurity site and on a plain location, respectively, marked by the squares in (c). The plain Cu spectrum shows the sharp onset of the surface state at $-440$ mV followed by some signal variations with sample voltage due to potential scattering of the surface-state electrons at nearby defects and step edges. In the spectra taken on the defects, the onset of the surface state has vanished. Instead, the typical signature of the Kondo resonance around zero bias is observed as a dip in the differential conductance. This dip is found to be much broader than was reported in the case of Co adsorbates. It must also be noted that we detected no dip in the $dI/dU$ spectra of buried impurities.

The theoretical results of Újsághy *et al.*[11] were used to fit the experimental curve in Fig. 3(a). Újsághy *et al.* as well as Plihal and Gadzuk[12] have both recovered a Fano-type line

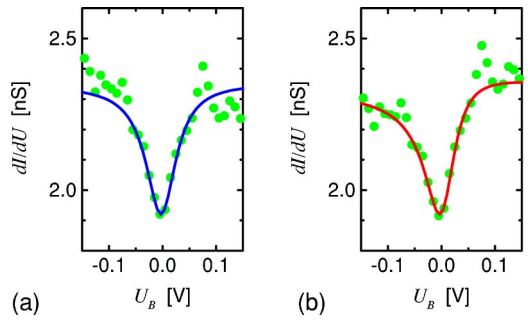


FIG. 4. (Color online) Fits of Eq. (2) to the experimental $dI/dU$ data. In (a) the spectrum is shown as it was measured, while in (b) an average background subtraction has been applied. The width of the dip is found to be $k_B T_K = 35 \pm 3$ meV (half width at half maximum).

shape for the Kondo feature, which requires an asymmetry parameter $q$ between 0 and 1 for a diplike appearance. The value of $q$ as well as the Kondo temperature $T_K$ of the specific system can be determined as a parameter from the fit of a Fano function,

$$\Delta\rho(U) = a\frac{q^2 - 1 + 2q\epsilon(U)}{\epsilon^2(U) + 1}, \tag{2}$$

where the bias dependence is contained in $\epsilon(U) = (eU + \epsilon_K)/k_B T_K$, and $\epsilon_K$ is the offset of the resonance from the Fermi energy. The fit was performed in the interval $[-90, +90]$ meV around the Fermi level. Two data sets were considered, one being identical to Fig. 3(a) and the other with the average slope $m$ of the spectrum ($m = -0.9$ nS/V) subtracted. The best fits to the original and modified spectra are plotted in Fig. 4. In both cases, the fit yields a half-width according to $k_B T_K = 35 \pm 3$ meV. The slope subtraction only affects the asymmetry parameter $q$ and the offset of the resonance from $E_F$, which is found to be $\epsilon_K = -2 \pm 5$ meV in the first case and $\epsilon_K = 4 \pm 4$ meV in the second. The half-width corresponds to a Kondo temperature of $T_K = 405 \pm 35$ K, which is nearly a factor of 8 larger than the $T_K$ of $\sim 54$ K measured with STS in the case of adatoms.[6,7] The asymmetry factor of the embedded Co was found to be $q = 0.03 \pm 0.03$ and $q = 0.20 \pm 0.05$, dependent on the application of a background slope subtraction. The embedded Co atom thus exhibits an asymmetry equal to or *smaller* than that determined from the measurement on Co adsorbates, which was reported to be $q = 0.18$.[7] This finding has to be contrasted to very recent theoretical results, which predict an increased $q$ value with reduced adsorbate-substrate distance for an adsorbed Kondo atom.[13] These predictions were made considering a distance variation of some ten picometers between adsorbate and matrix. Describing the embedded impurities which were examined in our experiment in terms of this adsorbate model, the change in distance approximately amounts to one atomic layer, which corresponds to $\Delta d \sim 209$ pm. Therefore, it appears questionable that the substrate-adsorbate distance should parametrize the $q$ variation alone, especially since the $s$ shell of the Co atom that

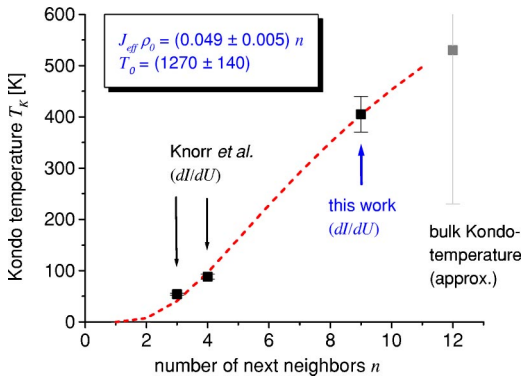


FIG. 5. (Color online) Fit of $T_K$ according to Eq. (1) to the experimental Kondo-temperature data. The simple scaling of $|J|\rho_0 \propto n$, the number of nearest neighbors (Ref. 7), is well followed by the present data points.

binds the atom to the substrate with metallic characteristic is always ignored in the calculations.

The high Kondo temperature measured for an embedded Co impurity can be explained using Eq. (1). As a simple model, Knorr *et al.* have proposed a scaling of $|J|\rho_0 \propto n$, where $n$ is the number of next-neighbor matrix atoms. This was based on Kondo-temperature data of adsorbates only. Together with their data, we can now check the validity of their assumption including *embedded* Co in Cu with $n=9$. A fit of Eq. (1) to the experimental data is shown in Fig. 5, taking into account $n=3$, 4, and 9. The value displayed for $T_K(n=12)=T_K^{\mathrm{bulk}}=530$ K represents an estimate for $T_K^{\mathrm{bulk}}$ extracted from experiment according to Ref. 14. The figure shows that a decent fit of this function to the discrete data points gained by STS can be found. The experimental value for $T_K$ determined in this work thus strongly supports the scaling relation proposed by Knorr and co-workers. Within that model, the STS data predict that $T_K^{\mathrm{bulk}}$ of dilute Co in Cu lies around 530 K.

In summary, we have characterized the Kondo properties of Co impurities in Cu(111)-based epitaxial dilute magnetic alloy films using a low-temperature STM. The Co defects are clearly visible via surface-state standing-wave patterns, even when lying inside the crystal, up to three layers below the surface. Surface-layer Co atoms show the characteristic dip at zero bias in the differential conductance arising from the Kondo effect. The width of the dip corresponds to a Kondo temperature of $T_K=405\pm35$ K, which substantially supports a scaling of $T_K$ with the number of next-neighbor matrix atoms as proposed by Knorr *et al.*

The authors acknowledge financial support from the DFG via SFB 602, project A3.

[1] *Magnetism*, edited by G. T. Rado and H. Suhl (Academic, New York, 1973), Vol. V, Chap. 4, p. 121.
[2] J. Kondo, Prog. Theor. Phys. **32**, 37 (1964).
[3] J. T. Li, W. D. Schneider, R. Berndt, and B. Delley, Phys. Rev. Lett. **80**, 2893 (1998).
[4] V. Madhavan, W. Chen, T. Jamneala, M. F. Crommie, and N. S. Wingreen, Science **280**, 567 (1998).
[5] T. Jamneala, V. Madhavan, W. Chen, and M. F. Crommie, Phys. Rev. B **61**, 9990 (2000).
[6] H. Manoharan, C. P. Lutz, and D. M. Eigler, Nature (London) **403**, 512 (2000).
[7] N. Knorr, M. A. Schneider, L. Diekhöner, P. Wahl, and K. Kern, Phys. Rev. Lett. **88**, 096804 (2002).
[8] M. A. Schneider, L. Vitali, N. Knorr, and K. Kern, Phys. Rev. B **65**, 121406(R) (2002).
[9] A. C. Hewson, *The Kondo Problem to Heavy Fermions* (Cambridge University Press, Cambridge, UK, 1993).
[10] S. Crampin, J. Phys.: Condens. Matter **6**, L613 (1994).
[11] O. Újsághy, J. Kroha, L. Szunyogh, and A. Zawadowski, Phys. Rev. Lett. **85**, 2557 (2000).
[12] M. Plihal and J. W. Gadzuk, Phys. Rev. B **63**, 085404 (2001).
[13] J. Merino and O. Gunnarsson, Phys. Rev. B **69**, 115404 (2004).
[14] R. Tournier and A. Blandin, Phys. Rev. Lett. **24**, 397 (1970).